12-11-2003

A close look at U (5) ↔ SU (3) transitional patterns in the interacting boson model

Feng Pan
Liaoning Normal University

J. P. Draayer
Louisiana State University

Yanan Luo
Louisiana State University

Recommended Citation

Pan, F., Draayer, J., & Luo, Y. (2003). A close look at U (5) ↔ SU (3) transitional patterns in the interacting boson model. *Physics Letters, Section B: Nuclear, Elementary Particle and High-Energy Physics, 576* (3-4), 297-302. https://doi.org/10.1016/j.physletb.2003.09.098

Available online at www.sciencedirect.com
SCIENCE DIRECT®
Physics Letters B 576 (2003) 297–302
PHYSICS LETTERS B
www.elsevier.com/locate/physletb

A close look at $U(5) \leftrightarrow SU(3)$ transitional patterns in the interacting boson model

Feng Pan [a,b], J.P. Draayer [b], Yanan Luo [b,c]

[a] *Department of Physics, Liaoning Normal University, Dalian 116029, PR China*
[b] *Department of Physics and Astronomy, Louisiana State University, Baton Rouge, LA 70803-4001, USA*
[c] *Department of Physics, Nankai University, Tianjin 300071, PR China*

Received 25 June 2003; accepted 19 September 2003

Editor: J.-P. Blaizot

Abstract

We study transitional patterns from the vibrational, $U(5)$, to the rotational, $SU(3)$, limit of the interacting boson model with a schematic Hamiltonian. The transitional behavior of low-lying energy levels, isomer shifts, E2 transition rates, and some other related quantities across the entire $U(5) \leftrightarrow SU(3)$ transitional region are studied in detail. The analysis shows that nuclei in the critical region are soft.

PACS: 21.60.Fw; 21.10.Re

Understanding shape phase transitions of a finite many-body system is paramount to understanding the system's underlying dynamics. The three possible phases that can occur in the interacting boson model for nuclei have been classified [1–3] as $U(5)$, $SU(3)$, and $O(6)$. The full scope of the transitional region can be characterized in terms of the Casten triangle [4]. The $U(5) \leftrightarrow SU(3)$ transitional description of the rare-earth nuclei Nd, Sm, Gd, and Dy was first reported in [5], including detailed results for most quantities of physical interest. Evidence for coexisting phases at low energy in the spherical-deformed transitional nucleus ^{152}Sm was also analyzed using $U(5) \leftrightarrow SU(3)$ transitional theory and the results show that the two phases coexist in a very small region of parameter space around the critical point [6]. Recently, since the discovery of the $X(5)$ symmetry in this region [7], the spherical to axially deformed shape phase transition has attracted further attention [8,9].

In this Letter, in order to take a close look at the $U(5) \leftrightarrow SU(3)$ shape phase transition, we study transitional patterns of many physical quantities, such as low-lying energy levels, isomer shifts, E2 transition rates, and some related quantities across the $U(5) \leftrightarrow SU(3)$ leg of the Casten triangle. No attempt is made to relate the results to realistic nuclei; rather, our purpose is to gain a better understanding the nature of the $U(5) \leftrightarrow SU(3)$ transition. In the study, the schematic Hamiltonian

$$\hat{H} = -c\left(x\hat{n}_s + \frac{(1-x)}{f(N)}\hat{Q}\cdot\hat{Q}\right), \tag{1}$$

E-mail address: daipan@dlut.edu.cn (F. Pan).

0370-2693
doi:10.1016/j.physletb.2003.09.098

which has been suggested as a suitable form for describing nuclei in this region is used, where the parameter $c > 0$, $0 \leqslant x \leqslant 1$ is the phase parameter, $f(N)$ is a linear function of the total number of bosons N, $\hat{n}_s = s^\dagger s$ is the number of s bosons, and $\hat{Q} = (s^\dagger \tilde{d} + d^\dagger \tilde{s}) - (\sqrt{7}/2)(d^\dagger \tilde{d})^{(2)}$. We note that $f(N) = 1$ was used in [6], while $f(N) = 4N$ was adopted in [7,10]. Also, the critical point x_c will be quite different for different choices of the function $f(N)$. Up to a constant, Hamiltonian (1) is equivalent to the one used in [5–7,10] with the relation $\zeta = 1 - x$.

In order to diagonalize the Hamiltonian (1), we expand eigenstates of (1) in terms of the $U(6) \supset SU(3) \supset SO(3)$ basis vectors $|N(\lambda\mu)KL\rangle$ as

$$|NL_\xi\rangle = \sum_{(\lambda\mu)K} C^{L_\xi}_{(\lambda\mu)K} \big|N(\lambda\mu)KL\big\rangle, \tag{2}$$

where the quantum number ξ indicating the ξth level with angular momentum quantum number L is introduced, and the $C^{L_\xi}_{(\lambda\mu)K}$ are expansion coefficients. Since the total number of bosons N is fixed for a given nucleus, the eigenstate given in (2) will also be denoted as $|L_\xi; x\rangle$ in the following, in which the value of the phase parameter x is explicitly shown. In our calculation, the orthonormalization process with respect to the band label K and the phase convention for the $SU(3) \supset SO(3)$ basis vectors proposed in [11,12] is used. By using analytic expressions for $U(6) \supset SU(3)$ reduced matrix element of the s-boson creation or annihilation operator [11] and an algorithm [12,13] for generating the $SU(3) \supset SO(3)$ Wigner coefficients, the eigenequation that simultaneously determines the eigenenergy and the corresponding set of the expansion coefficients $\{C^{L_\xi}_{(\lambda\mu)K}\}$ can be established.

To explore the transitional patterns, we fix the total number of bosons at $N = 10$ and allow the phase parameter x to vary in the closed interval $[0, 1]$. The functional form of $f(N)$ is chosen to be the same as that used in [7] with $f(N) = 4N$ unless otherwise specifically noted. Some low-lying energy levels as a function of x are shown in Fig. 1 from which one can see that there is a minimum in the excitation energy around $x \sim 0.41$–0.46, which corresponds to the spherical-deformed shape coexistence region which is also referred to as the critical (phase transition) region. It can also be seen that the minimum is not exactly the same for all the levels, but all fall within the spherical-deformed shape coexistence region.

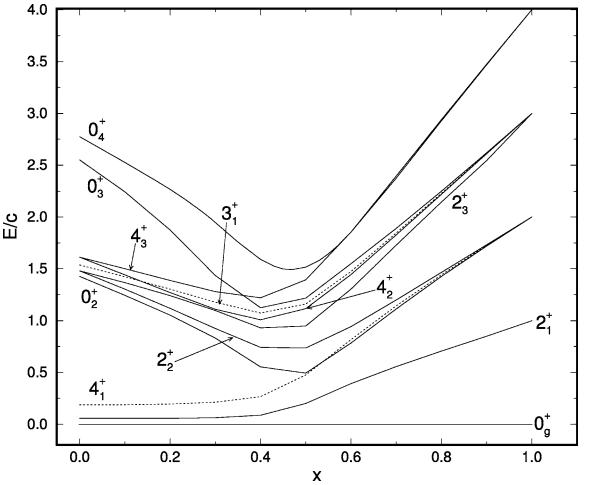

Fig. 1. Some low-lying energy levels across the transitional region, where $x = 0$ point corresponds to the axially deformed shape with rotational spectrum and $x = 1$ point to the spherical shape with vibrational spectrum.

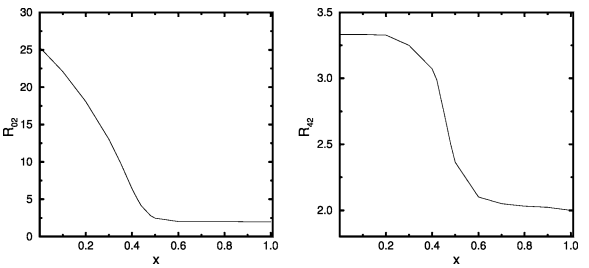

Fig. 2. Energy ratios R_{02} and R_{42} as functions of the transitional parameter x.

Two energy ratios, $R_{02} = E_{0_2^+}/E_{2_1^+}$ and $R_{42} = E_{4_1^+}/E_{2_1^+}$, are shown as a function of x in Fig. 2. The ratio R_{02} drops rather precipitously from the rotational limit, $R_{02} \sim 25$, to the vibrational limit, $R_{02} \sim 2$, over the range $0 \leqslant x < \sim 0.5$ and then remains at the vibrational limit for $x > \sim 0.5$. While the ratio R_{42} drops rather smoothly as a function of x from the rotational limit, $R_{42} = 10/3$ when $0 \leqslant x < \sim 0.3$, to the vibrational limit, $R_{42} = 2$ when $\sim 0.6 < x \leqslant 1$. The sharpest change occurs around the critical point $x_c \sim 0.46$ when the absolute value of the derivative of R_{42} with respect to x reaches the maximal value. To show how the transition occurs in the ground state, the amplitudes $|C_{(\lambda\mu)}|^2$ are plotted as functions of x

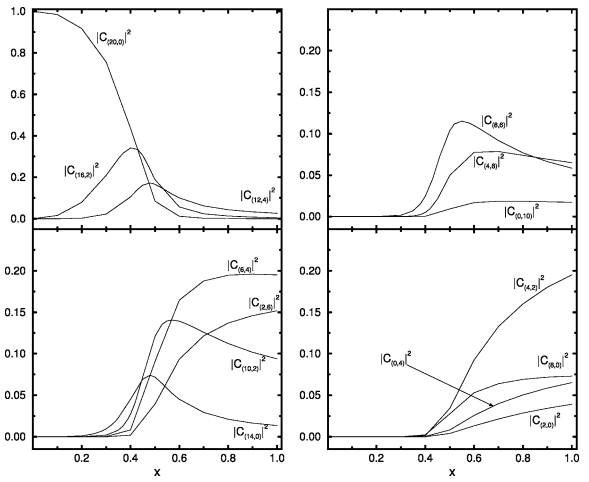

Fig. 3. Amplitudes $|C_{(\lambda\mu)}|^2$ of the ground state as functions of the transitional parameter x.

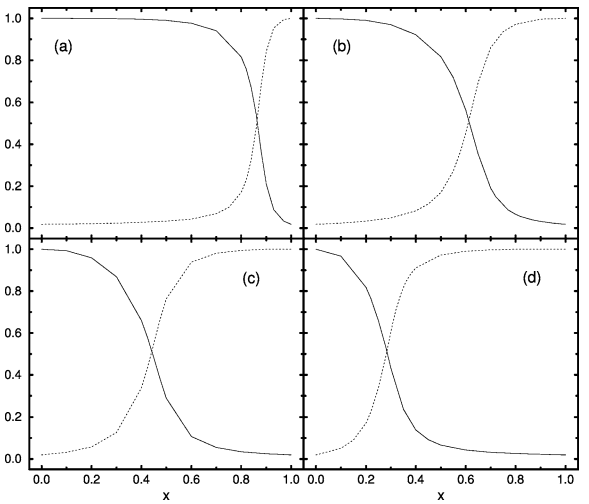

Fig. 4. Overlaps of the ground state wavefunction, where the full line shows the overlap $|\langle 0_g^+; x=0|0_g^+; x\rangle|$, and the dotted line shows the overlap $|\langle 0_g^+; x=1|0_g^+; x\rangle|$. (a) $f(N)=0.5N$; (b) $f(N)=2N$; (c) $f(N)=4N$; (d) $f(N)=8N$.

in Fig. 3, which indicate that the most rapid changes in these amplitudes also occur within the coexistence region.

In order to explore the exact nature of the critical point with different choices for the linear function $f(N)$, overlaps $|\langle 0_g^+; x|0_g^+; x_0\rangle|$ with $x_0 = 0$ or 1 as suggested in [7] with $f(N) = 0.5N$, $2N$, $4N$, and $8N$, respectively, were calculated. The results are shown in Fig. 4, from which it can be clearly seen that the

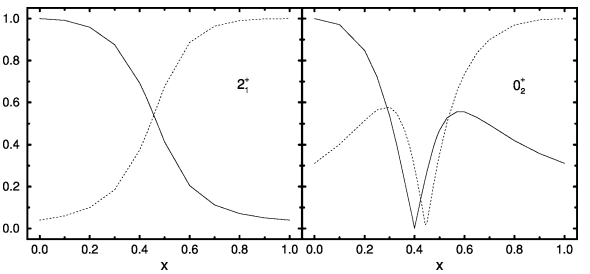

Fig. 5. Typical overlaps of two excited states, where the full line shows the overlap $|\langle L_\xi^+; x=0|L_\xi^+; x\rangle|$, and the dotted line shows the overlap $|\langle L_\xi^+; x=1|L_\xi^+; x\rangle|$.

critical (crossing) point changes with different choices of the function $f(N)$. The larger the $f(N)$ value, the smaller the critical point value x_c. This conclusion confirms the early result shown in [6], in which the critical point value is very large with $x_c = 0.974$ corresponding to $f(N) = 1$, while for $x_c \sim 0.46$ when $f(N) = 4N$ with $N = 10$ is used [7,10]. It should also be pointed out that the critical point may differ from one excited state to the next for the same choice of $f(N)$. Our calculation shows that the critical points for 0_g^+, 2_1^+, and 4_1^+ are almost the same, but they are somewhat different for 2_3^+ and 3_1^+. It should also be noted that curves of the overlaps $|\langle L_\xi^+; x|L_\xi^+; x_0\rangle|$ with $x_0 = 0$ or 1 even become irregular for 0_2^+, 2_2^+, 4_2^+, and 0_3^+. Typical examples of these curves for higher excited states are shown in Fig. 5, which indicate that the critical point for higher excited states may be quite different from that of the ground state. This behavior will be seen in other observables such as E2 transition rates since the critical behavior of the initial and final states may quite different from that of ground state.

Another quantity that is sensitive to the transition is the isomer shift defined by [5]

$$\delta\langle r^2\rangle = \alpha_0\big(\langle 2_1^+; x|\hat{n}_d|2_1^+; x\rangle - \langle 0_g^+; x|n_d|0_g^+; x\rangle\big), \quad (3)$$

where α_0 is a constant. Fig. 6 displays the isomer shift as a function of x. The largest absolute value of the derivative of the isomer shift with respect to x also occurs around the critical point $x_c \sim 0.46$.

The E2 operator is simply chosen as

$$T(\mathrm{E2}) = q_2\hat{Q}, \quad (4)$$

where q_2 is the effective charge. Various $B(\mathrm{E2})$ values and ratios among the low-lying levels were studied.

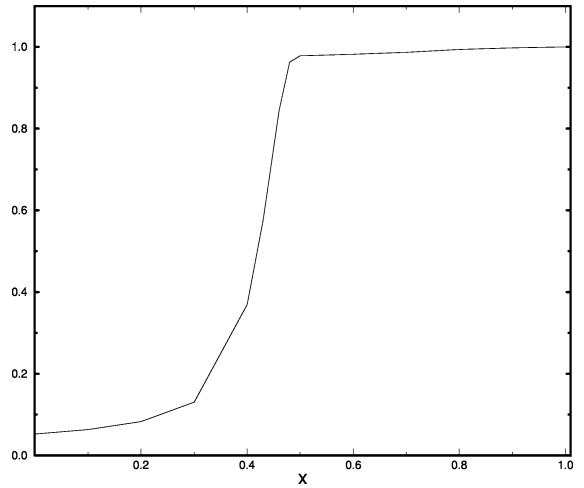

Fig. 6. The isomer shift $\delta\langle r^2\rangle/\alpha_0$ defined by Eq. (3) as a function of the transitional parameter x.

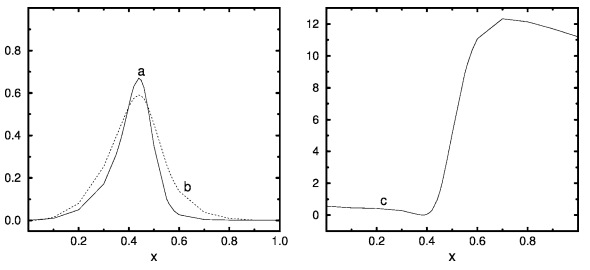

Fig. 7. Some $B(\mathrm{E2})/q_2^2$ values as functions of the transitional parameter x, where curve a represents $B(\mathrm{E2}; 2_3^+ \to 0_g^+)/q_2^2$, curve b represents $B(\mathrm{E2}; 2_3^+ \to 2_1^+)/q_2^2$, and curve c represents $B(\mathrm{E2}; 2_3^+ \to 0_2^+)/q_2^2$.

Some $B(\mathrm{E2})$ values and ratios were found to be sensitive to the shape phase transition. Fig. 7 provides three $B(\mathrm{E2})$ values, $B(\mathrm{E2}; 2_3^+ \to 0_g^+)$, $B(\mathrm{E2}; 2_3^+ \to 2_1^+)$, and $B(\mathrm{E2}; 2_3^+ \to 0_2^+)$. There is a small peak around $x \sim 0.44$ for $B(\mathrm{E2}; 2_3^+ \to 0_g^+)$ and $B(\mathrm{E2}; 2_3^+ \to 2_1^+)$, while there is a saddle point around $x \sim 0.38$ for $B(\mathrm{E2}; 2_3^+ \to 0_2^+)$. As seen previously, the peaks and saddle points in these $B(\mathrm{E2})$ values are different from the critical point of the ground state due to different critical behavior of the excited states. Fig. 8 provides six $B(\mathrm{E2})$ ratios, $B(\mathrm{E2}; 2_2^+ \to 0_g^+)/B(\mathrm{E2}; 2_2^+ \to 2_1^+)$, $B(\mathrm{E2}; 2_2^+ \to 2_1^+)/B(\mathrm{E2}; 2_1^+ \to 0_g^+)$, $B(\mathrm{E2}; 2_3^+ \to 0_2^+)/B(\mathrm{E2}; 2_1^+ \to 0_g^+)$, $B(\mathrm{E2}; 2_3^+ \to 0_1^+)/B(\mathrm{E2}; 2_3^+ \to 0_2^+)$, $B(\mathrm{E2}; 2_3^+ \to 2_1^+)/B(\mathrm{E2}; 2_3^+ \to 0_g^+)$, and

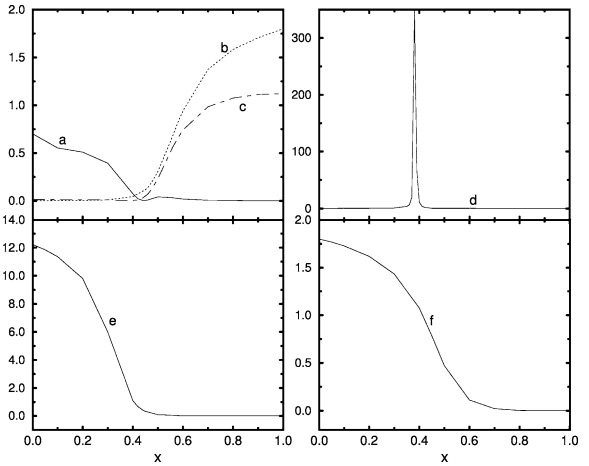

Fig. 8. Some $B(\mathrm{E2})$ ratios as functions of the transitional parameter x, where curve a represents $B(\mathrm{E2}; 2_2^+ \to 0_g^+)/B(\mathrm{E2}; 2_2^+ \to 2_1^+)$, curve b represents $B(\mathrm{E2}; 2_2^+ \to 2_1^+)/B(\mathrm{E2}; 2_1^+ \to 0_g^+)$, curve c represents $B(\mathrm{E2}; 2_3^+ \to 0_2^+)/B(\mathrm{E2}; 2_1^+ \to 0_g^+)$, curve d represents $B(\mathrm{E2}; 2_3^+ \to 0_1^+)/B(\mathrm{E2}; 2_3^+ \to 0_2^+)$, curve e represents $B(\mathrm{E2}; 2_3^+ \to 2_1^+)/B(\mathrm{E2}; 2_3^+ \to 0_g^+)$, and curve f represents $B(\mathrm{E2}; 3_1^+ \to 2_1^+)/B(\mathrm{E2}; 3_1^+ \to 4_1^+)$.

$B(\mathrm{E2}; 3_1^+ \to 2_1^+)/B(\mathrm{E2}; 3_1^+ \to 4_1^+)$. These ratios all undergo noticeable changes within the coexistence region. The most distinctive signature is shown in $B(\mathrm{E2}; 2_3^+ \to 0_1^+)/B(\mathrm{E2}; 2_3^+ \to 0_2^+)$, in which there is a giant peak around $x \sim 0.38$. This giant peak shown by curve d in Fig. 8 is due mainly to the near vanishing of the denominator, $B(\mathrm{E2}; 2_3^+ \to 0_2^+)$, shown by curve c in Fig. 7.

In order to study shape of nuclei around the critical point, we use the relation between the Bohr variables (β, γ) of the collective model and the (λ, μ) labels that define the irreducible representation of the $SU(3)$ [14]. In this algebraic approach, the Bohr variable β can be expressed as a function of $SU(3)$ Casimir operator of the second order with

$$\hat{\beta} = \beta_0 \sqrt{\hat{C}_2\big(SU(3)\big) + 3} \tag{5}$$

with

$$\beta_0 = \sqrt{\frac{4\pi}{5Ar_0^2}}, \tag{6}$$

where A denotes the number of like particles and r_0^2 is a dimensionless mean square radius [14]. The variable γ in radian measure can also be expressed

Table 1
Expectation values $\bar{\beta}/\beta_0$ and $\bar{\gamma}$ of the ground state, and the corresponding root-mean-square deviations $\Delta(\beta)/\beta_0$ and $\Delta(\gamma)$, respectively, for some specific values of x

	$x=0.0$	$x=0.1$	$x=0.2$	$x=0.3$	$x=0.4$	$x=0.46$
$\bar{\beta}/\beta_0$	21.52	21.47	20.27	20.71	19.06	16.64
$\Delta(\beta)/\beta_0$	0.000	0.357	0.835	1.529	2.737	3.688
$\bar{\gamma}$	0.040	0.042	0.049	0.068	0.123	0.212
$\Delta(\gamma)$	0.000	0.0124	0.0292	0.2600	0.111	0.177
	$x=0.5$	$x=0.6$	$x=0.7$	$x=0.8$	$x=0.9$	$x=1.0$
$\bar{\beta}/\beta_0$	14.71	11.97	10.90	10.33	9.97	9.71
$\Delta(\beta)/\beta_0$	3.884	3.496	3.229	3.088	3.000	2.941
$\bar{\gamma}$	0.287	0.393	0.430	0.447	0.456	0.462
$\Delta(\gamma)$	0.209	0.230	0.234	0.235	0.236	0.237

as a functional of the second and third order Casimir operators. For simplicity, it can be written as

$$\hat{\gamma} = \tan^{-1}\left(\frac{\sqrt{3}\,(\hat{\mu}+1)}{2\hat{\lambda}+\hat{\mu}+3}\right). \tag{7}$$

In (7), $\hat{\lambda}$ and $\hat{\mu}$ should be regarded as operators, of which the results are the usual λ and μ values when they are applied to the basis vector of $SU(3)$. Using the definitions (5) and (6), we can calculate the expectation values, $\bar{\beta} = \langle 0_g^+; x|\hat{\beta}|0_g^+; x\rangle$, and $\bar{\gamma} = \langle 0_g^+; x|\hat{\gamma}|0_g^+; x\rangle$ in the ground state and the corresponding root mean square deviations defined by

$$\pm\Delta(\beta) = \pm\sqrt{\langle 0_g^+; x|(\hat{\beta}-\bar{\beta})^2|0_g^+; x\rangle},$$
$$\pm\Delta(\gamma) = \pm\sqrt{\langle 0_g^+; x|(\hat{\gamma}-\bar{\gamma})^2|0_g^+; x\rangle}. \tag{8}$$

The results are shown in Table 1 and Fig. 9. These quantities can be used to display the uncertainty in the shape as a function of x. It is obvious that $\Delta(\beta)$ and $\Delta(\gamma)$ are zero in the rotational limit ($x=0$) that corresponds to a definite shape, while the shape is less well defined as x moves away from zero. The values of $\Delta(\beta)$ and $\Delta(\gamma)$ are not small in the vibrational limit ($x=1$) due to the quadrupole vibration being non-negligible. As can be seen from Fig. 9, there are also obvious changes in $\bar{\beta}$ and $\bar{\gamma}$ in the critical region around $x \sim 0.46$. Over the whole range, the magnitude of the change in $\bar{\gamma}$ is small. From Table 1, it can be seen that $\Delta(\beta)$ reaches the maximum value around $x \sim 0.5$ which deviates a little from the critical point $x_c \sim 0.46$ of the ground state, but is still near the critical region. This distinctive signature shows that nucleus is the softest in the critical region. This fact

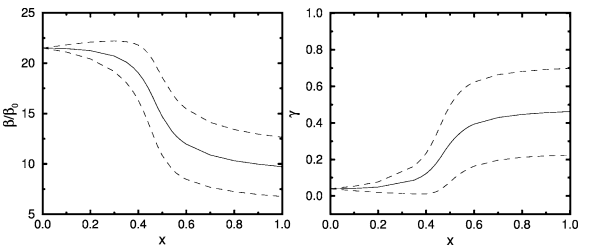

Fig. 9. The ground state expectation values of Bohr variables $\bar{\beta}/\beta_0$ and $\bar{\gamma}$ and the corresponding root mean square deviations $\Delta(\beta)/\beta_0$ and $\Delta(\gamma)$, where the full line indicates the expectation value $\bar{\beta}/\beta_0$ or $\bar{\gamma}$, while the dotted lines show the corresponding root mean square deviations $\pm\Delta(\beta)/\beta_0$ or $\pm\Delta(\gamma)$.

can help us to understand why there is a saddle region in most excited levels; namely, a nucleus in this region is comparatively soft and therefore its shape can be changed easily with very little energy. Hence, nuclei in this region can easily be excited, which results in relatively smaller energy gaps in this soft critical region. The same calculations for 0_2^+ state are shown in Table 2.

In conclusion, transitional patterns from the vibrational, $U(5)$, to the rotational, $SU(3)$, limit of the interacting boson model with a schematic Hamiltonian have been studied. The transitional behavior of low-lying energy levels, isomer shifts, E2 transition rates, and related quantities over the whole $U(5) \leftrightarrow SU(3)$ transitional region were explored. The results show that there are many distinctive signatures in the energy levels, wavefunctions, isomer shifts, $B(\mathrm{E2})$ values and ratios, and expectation values of shape variables near the critical point. Generally speaking, the critical behavior of excited states are different from

Table 2
Expectation values $\bar{\beta}/\beta_0$ and $\bar{\gamma}$ of 0_2^+ state, and the corresponding root-mean-square deviations $\Delta(\beta)/\beta_0$ and $\Delta(\gamma)$, respectively, for some specific values of x

	$x=0.0$	$x=0.1$	$x=0.2$	$x=0.3$	$x=0.4$	$x=0.45$	$x=0.46$
$\bar{\beta}/\beta_0$	18.68	18.61	18.28	17.21	14.89	14.67	14.76
$\Delta(\beta)/\beta_0$	0.000	0.667	1.578	2.949	4.637	5.366	5.474
$\bar{\gamma}$	0.140	0.141	0.150	0.189	0.299	0.314	0.311
$\Delta(\gamma)$	0.000	0.028	0.068	0.140	0.241	0.268	0.270
	$x=0.5$	$x=0.55$	$x=0.6$	$x=0.7$	$x=0.8$	$x=0.9$	$x=1.0$
$\bar{\beta}/\beta_0$	15.22	15.33	14.97	13.89	12.98	12.32	11.87
$\Delta(\beta)/\beta_0$	5.651	5.543	5.423	5.281	5.154	5.027	4.914
$\bar{\gamma}$	0.286	0.269	0.270	0.293	0.320	0.344	0.362
$\Delta(\gamma)$	0.269	0.255	0.244	0.232	0.233	0.234	0.235

that of ground state, which may lead to different critical point for some physical quantities. In comparison with the result shown in [9], a nucleus with $X(5)$ symmetry can be described approximately by the $U(5) \leftrightarrow SU(3)$ transitional theory within the critical region. Our analysis also shows that shapes of nucleus in the critical region is not well defined; that is, a nucleus with $X(5)$ symmetry is soft.

Acknowledgements

We are grateful to Dr. N.V. Zamfir for helpful discussions. This work was supported by the US National Science Foundation (0140300) and by the Natural Science Foundation of China (10175031).

References

[1] A. Arima, F. Iachello, Ann. Phys. (N.Y.) 99 (1976) 253.
[2] A. Arima, F. Iachello, Ann. Phys. (N.Y.) 111 (1978) 201.
[3] A. Arima, F. Iachello, Ann. Phys. (N.Y.) 123 (1979) 468.
[4] R.F. Casten, in: F. Iachello (Ed.), Interacting Bose–Fermi System, Plenum, New York, 1981.
[5] O. Scholten, F. Iachello, A. Arima, Ann. Phys. (N.Y.) 115 (1978) 325.
[6] F. Iachello, N.V. Zamfir, R.F. Casten, Phys. Rev. Lett. 81 (1998) 1191.
[7] F. Iachello, Phys. Rev. Lett. 87 (2001) 052502.
[8] N.V. Zamfir, P. von Brentano, R.F. Casten, J. Jolie, Phys. Rev. C 66 (2002) 021304(R).
[9] J.E. Garcia-Ramos, J.M. Arias, J. Barea, A. Frank, nucl-th/0304008.
[10] V. Werner, P. von Brentano, R.F. Casten, J. Joile, Phys. Lett. B 527 (2002) 55.
[11] G. Rosensteel, Phys. Rev. C 41 (1990) 730.
[12] J.P. Draayer, Y. Akiyama, J. Math. Phys. 14 (1973) 1904.
[13] Y. Akiyama, J.P. Draayer, Comput. Phys. Commun. 5 (1973) 405.
[14] O. Castaños, J.P. Draayer, Y. Leschber, Z. Phys. A 329 (1988) 33.